Tetrahedron 74 (2018) 465–476

Contents lists available at ScienceDirect

Tetrahedron

journal homepage: www.elsevier.com/locate/tet

Turn-on fluorescence sensor for mono- and di-phosphonic acid derivatives using anthracene-based diamidine and its detection of amidinium-phosphonate and amidinium formation

Takahiro Kusukawa*, Hitoshi Nagano, Keita Nakaguchi, Shota Takeshita, Yuya Harumoto

Department of Chemistry and Materials Technology, Graduate School of Science and Technology, Kyoto Institute of Technology, Matsugasaki, Sakyo-ku Kyoto 606-8585, Japan

ARTICLE INFO

Article history:
Received 31 October 2017
Received in revised form
4 December 2017
Accepted 6 December 2017
Available online 7 December 2017

Keywords:
Amidinium-phosphonate
Amidinium
Fluorescence
Phosphonic acid recognition

ABSTRACT

The fluorescence detection of di-phosphonic acid and mono-phosphonic acid derivatives using the anthracene-based diamidine **1** has been investigated. The diamidine **1** forms 1:1 and 1:2 complexes with the di-phosphonic acid and mono-phosphonic acid derivatives, respectively, and showed a blue fluorescence (λ_{em} = 432–442 nm) in a DMSO solution. The formation of amidinium-phosphonate (complex formation) and dissociated amidinum (λ_{em} = 468 nm as a broad band) were distinguished by the difference in the fluorescence wavelength, and confirmed by DOSY NMR spectroscopy and TD-DFT calculations. The formation of a 1:2 complex with diamidine **1** and methylphosphonic acid having additional intermolecular hydrogen-bonding between the methylphosphonic acids is proposed.

1. Introduction

The development of fluorogenic chemosensors for phosphorus-related oxoacids (oxoanions) is of particular interest due to their applications in the chemical, biological and environmental sciences.[1] Although there are numerous reports of fluorogenic chemosensors for "phosphoric acids (phosphate)",[1a] only a few examples of fluorogenic chemosensors for "phosphonic acids (phosphonate)" have been reported.[2] The phosphonic acid derivatives have a broad range of applications[3] where they find utility, such as in bone cancer treatments and care for diseases related to osteoporosis.

The amidine is known to bind with oxoacids, such as carboxylic acids, phosphonic acids, phosphoric acids and sulfonic acids, and forms salt bridges having twitter ionic charges.[4] Due to the formation of the twitter ionic charges, the hydrogen bond of the amidinium-oxoanion salt bridge shows a stronger binding even in polar solvents (i.e., charge-assisted hydrogen bond[4a]). Recently, we reported the fluorescence detection of α,ω-dicarboxylic acids using an anthracene-based diamidine **1** in a DMSO solution and succeeded in the quantification of the amount of dicarboxylic acid in human urine as a "turn-on" type fluorescence sensor.[5] In this system, the formation of cationic charges after the recognition of the dicarboxylic acids suppresses the PET (photoinduced electron transfer[6]) processes and consequently "turns-on" the fluorescence after the recognition of carboxylic acids (formation of amidinium-carboxylate salt bridge, Scheme 1).

We now report the fluorescence detection of "phosphonic acid derivatives" using the anthracene-based diamidine **1**. The anthracene-based diamidine **1** recognize mono- and di-phosphonic acid derivatives by the formation of "amidinium-phosphonate" salt bridges and consequently turn-on the fluorescence. To compare the recognition ability between "dicarboxylic acids" and "diphosphonic acid derivatives", we examined the recognition of α,ω-diphosphonic acid having two hydroxyl groups for one phosphorous atom (i.e., 1,8-octanediphosphonic acid). However, the precipitation of the formed complexes was observed and could not characterize the structure of the binding complex using NMR spectroscopy. To increase the solubility of the formed complexes, we synthesized new diphosphonic acid diethyl esters **2** having two solubilizing ethyl groups. The formation of 1:1 complexes of diamidine **1** and diphosphonic acid diethyl esters **2** was analyzed by ^{1}H, ^{31}P NMR, DOSY NMR and fluorescence spectroscopies. The formation of the "stable 1:1 complex **1•2**" or "dissociated amidinium **1•2H**$^{+}$" was also characterized by DOSY NMR spectroscopy and the differences

* Corresponding author.
E-mail address: kusu@kit.ac.jp (T. Kusukawa).

https://doi.org/10.1016/j.tet.2017.12.011
0040-4020/

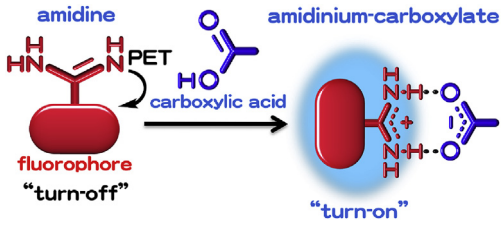

Scheme 1. Schematic representation of the formation of amidinium-carboxylate salt bridge and its fluorescence characters.

in the wavelengths of the fluorescence spectra (Scheme 2).

Surprisingly, the formation of 1:2 complexes **1**•(**3**)$_2$ was observed for the recognition of the mono-phosphonic acids **3** which have two hydroxyl groups on the phosphorous atom. Similar 1:2 complexes of diamidine **1** with mono-carboxylic acids have never been observed and form only the dissociated amidinium **1**•2**H**$^+$. In the case of the mono-phosphonic acid binding, the formation of 1:2 complexes **1**•(**3**)$_2$ is achieved by the formation of additional intermolecular hydrogen bonding between the phosphonic acids after formation of the amidinium-phosphonate salt bridges.

2. Results and discussion

2.1. Synthesis of diphosphonic acid derivatives

The diphosphonic acid diethyl esters **2** were prepared according to Scheme 3. The tetraethyl diphosphonate derivatives **5** were prepared from the corresponding dibromide by the Arbuzov reaction (refluxing in P(OEt)$_3$) or cross-coupling conditions (NiCl$_2$/P(OEt)$_3$). The obtained tetraethyl diphosphonate derivatives **5** were refluxed with anhydrous LiBr in 2-hexanone and the precipitates of the dilithium-diphosphonate derivatives **6** were collected by centrifugation. The diphosphonic acid diethyl esters **2** were prepared from the corresponding dilithium-diphosphonates **6** by the treatment with an ion exchange resin.

2.2. Binding experiments of anthracene-based diamidine *1* with diphosphonic acid diethyl esters (*2a*, *2b*)

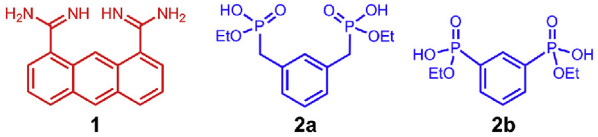

To investigate the recognition ability of the diamidine **1** toward the diphosphonic acid derivatives, we observed the ^{1}H NMR and DOSY NMR spectra for the complexation of diamidine **1** with the structurally slightly rigid diphosphonic acid diethyl esters (**2a**, **2b**). The formation of the 1:1 complex **1•2a** was achieved by mixing the DMSO-d_6 solution (1.89 mM) of **1** and **2a** (*m*-xylylene diphosphonic acid diethyl ester). The ^{1}H NMR spectrum of the obtained solution showed the characteristic upfield and downfield shifts with respect to those of **1** and **2a**, respectively (Fig. 1 and Fig. S1). The downfield shift of the amidine unit (H^a-H^c, H^e) and the upfield shift of the phosphonic acid unit (H^A-H^C, H^E, H^F) in the ^{1}H NMR indicated the formation of a cationic charge and an anionic charge in each unit after complexation. The resonance of the NH protons was observed at 11.9 and 9.7 ppm (Fig. 1b). Based on the comparison of the formation of "amidinium-carboxylate" binding complexes,[5] these NH proton signals strongly indicated the fomation of "amidinium-phosphonate" salt bridges (i.e., formation of a stable complex).

Additional proof of the formation of **1•2a** was obtained from the DOSY NMR spectroscopy. The ^{1}H DOSY spectra showed that the diffusion coefficient of complex **1•2a** is lower than those of the corresponding free building blocks (**1**, **2a**), confirming the formation of the larger-sized complex (Fig. 2). The molecular volume of **1•2a** derived from the observed diffusion coefficient (V = 1062 Å^3) is slightly greater than the sum of the volumes of the free building blocks (**1**: V = 280 Å^3, **2a**: V = 352 Å^3), but smaller than the volume after the formation of the 2:2 complex **1**$_2$•(**2a**)$_2$ (V_{calc} = 1264 Å^3), which indicated the formation of the stable 1:1 complex (Fig. 2, Table 1).[7] The complexation of diamidine **1** with the *m*-phenylene diphosphonic acid diethyl ester **2b** also showed the formation of the stable 1:1 complex **1•2b** in DMSO, which was confirmed by ^{1}H NMR and DOSY NMR spectroscopies (Figs. S2 and S26, Table 1).

2.3. Binding experiments of diamidine *1* with α,ω-diphosphonic acid diethyl esters (*2c*-*2h*)

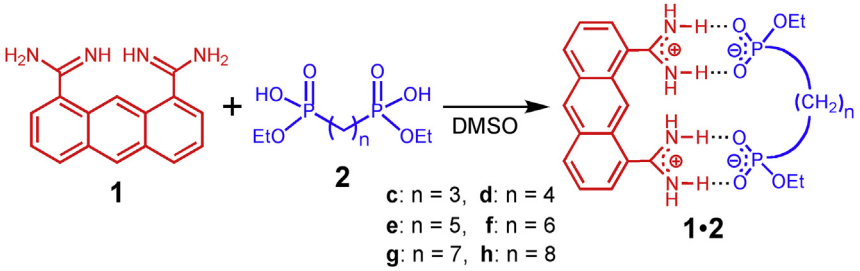

To compare the recognition ability of the diamidine **1** toward "diphosphonic acid derivatives" and "dicarboxylic acids", we examined the recognition of the conformationally flexible α,ω−diphosphonic acid derivatives. However, after the complexation of diamidine **1** with α,ω-diphosphonic acid, which has two hydroxyl groups for one phosphorous atom (i.e. 1,8-octanediphosphonic acid), precipitation was observed from the DMSO solution. To increase the solubility of the formed complexes, we synthesized α,ω−diphosphonic acid diethyl esters **2c**-**2h** which have soluble ethyl groups (protection of the hydroxyl group to inhibit the formation of a higher aggregate). The formation of the 1:1 complex **1•2g** (n = 7, 0.95 mM) was achieved by mixing the DMSO-d_6 solution of both components. After complexation, the ^{1}H NMR spectrum of the obtained solution showed the characteristic upfield and downfield shifts with respect to those of **1** and **2g**, and

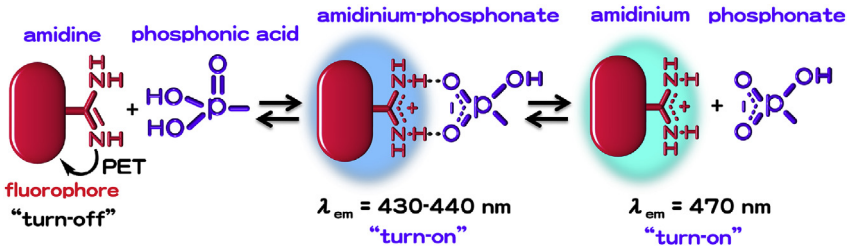

Scheme 2. Schematic representation of the formation of amidinium-phosphonate and dissociated amidinium, and their fluorescence characters.

resonance of the NH protons was also observed at 12.7 and 9.6 ppm, respectively, which indicated the formation of the stable complex (Fig. 3b and Fig. S7). Additional proof of the formation of **1•2g** (n = 7) in the solution state was also obtained from DOSY NMR spectroscopy. The DOSY spectra showed that the diffusion coefficient of complex **1•2g** is lower than those of the corresponding free building blocks (**1**, **2g**), confirming the formation of the larger-sized complex (Fig. 4). The molecular volume of **1•2g** derived from the observed diffusion coefficient (V = 932 Å^3) is slightly greater than the sum of the volumes of the free building blocks (**1**: V = 297 Å^3, **2g**: V = 372 Å^3), which indicated the formation of the stable 1:1 complex (Table 2).

For the complexation of diamidine **1** with the diphosphonic acid diethyl esters **2c**-**2f** (n = 3–6) and **2h** (n = 8), the ^{1}H NMR spectra of the formed complexes showed reasonable upfield and downfield shifts indicating the formation of stable complexes (Figs. S4–S8). For the 1:1 complexes, **1•2d**, **1•2f**, and **1•2h**, similar diffusion coefficients (molecular volume) compared to the formation of **1•2g** were observed by the DOSY NMR spectroscopy which indicated the formation of stable 1:1 complexes (Table 2). In the case of the diphosphonic acid diethyl ester **2c**, which has a slightly shorter methylene chain length compared to the distances between the

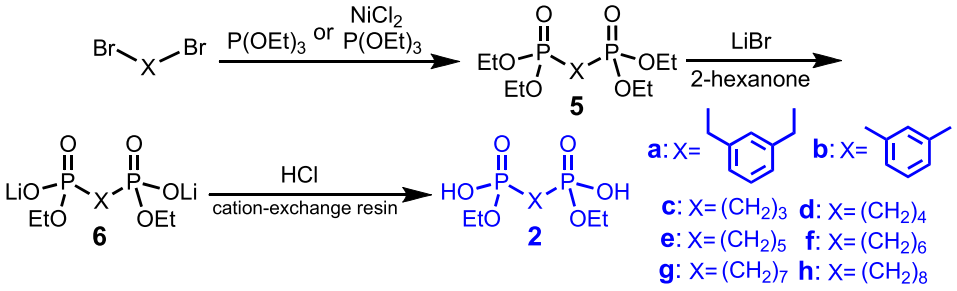

Scheme 3. Synthesis of diphosphonic acid diethyl esters **2**.

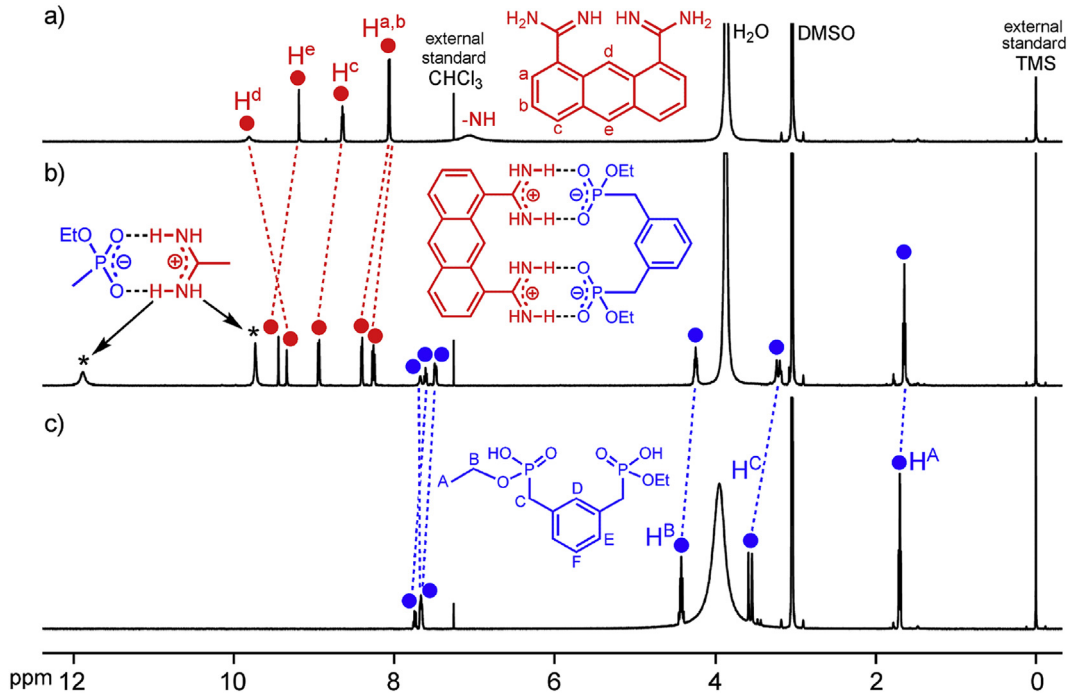

Fig. 1. ^{1}H NMR spectra (1.89 mM in DMSO-d_6, 298 K) of a) diamidine **1**, b) **1•2a** obtained by mixing equimolar solutions of **1** and **2a**, and c) diphosphonic acid diethyl ester **2a**.

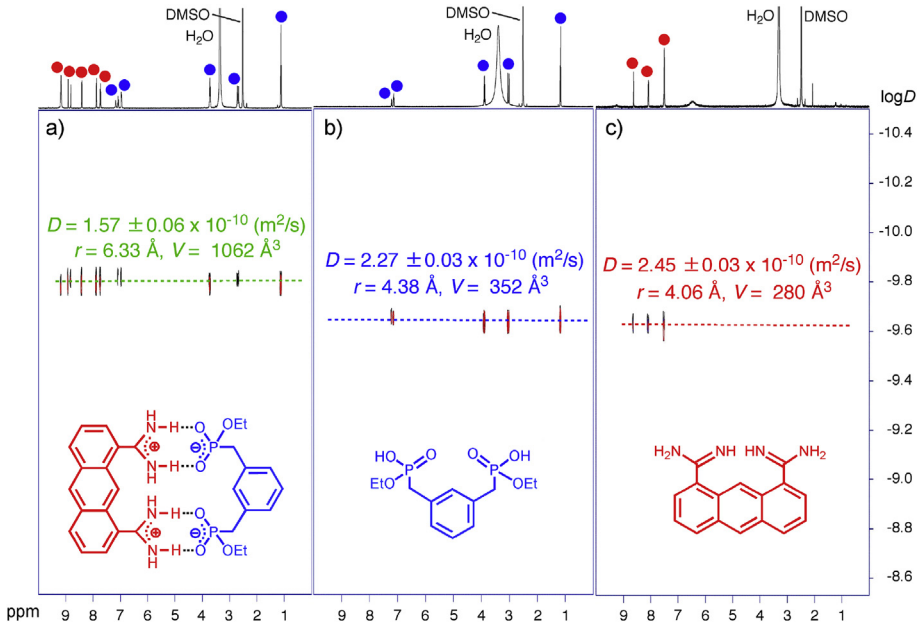

Fig. 2. [1]H DOSY spectra (1.89 mM in DMSO-d_6, 25 °C, diffusion time Δ = 200 ms) of a) complex **1•2a**, b) diphosphonic acid diethyl ester **2a**, c) diamidine **1**.

Table 1
Comparison of diffusion coefficients, molecular radii and volumes.[a]

Compounds	D (m^2 s^{-1})	r_H (Å)	V (Å^3)
1	$2.45 \pm 0.03 \times 10^{-10}$	4.06	280
2a	$2.27 \pm 0.03 \times 10^{-10}$	4.38	352
1•2a	$1.57 \pm 0.06 \times 10^{-10}$	6.33	1062
2b	$2.37 \pm 0.02 \times 10^{-10}$	4.20	310
1•2b	$1.70 \pm 0.06 \times 10^{-10}$	5.85	839

[a] Diffusion coefficients were recorded at 298 K in DMSO-d_6 (1.89 mM, diffusion time Δ = 200 ms), and the molecular radii were calculated using the Stokes-Einstein equation.

two amidino groups of **1**, different diffusion coefficients were separately observed indicating the formation of the slightly weaker 1:1 complex **1•2c**. Also, in the case of **1•2e** (n = 5), precipitation was observed within several hours after complexation, and could not observed by DOSY NMR spectroscopy (Figs. S27–S30).

2.4. Fluorescence detection of diphosphonic acid diethyl esters **2**: detection of amidinium-phosphonate and amidinium formation

To demonstrate the recognition ability of the diamidine **1**, we observed the fluorescence spectra of the diamidine **1** with the

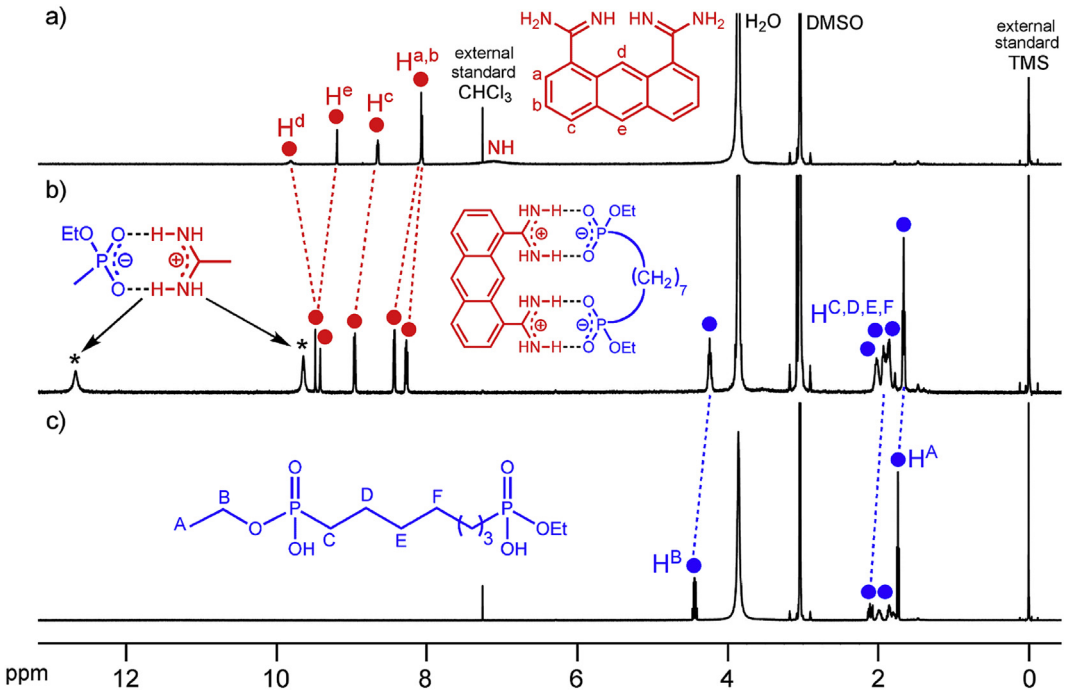

Fig. 3. [1]H NMR spectra (0.95 mM in DMSO-d_6, 298 K) of a) diamidine **1**, b) **1•2g** obtained by mixing equimolar solutions of **1** and **2g**, and c) diphosphonic acid diethyl ester **2g**.

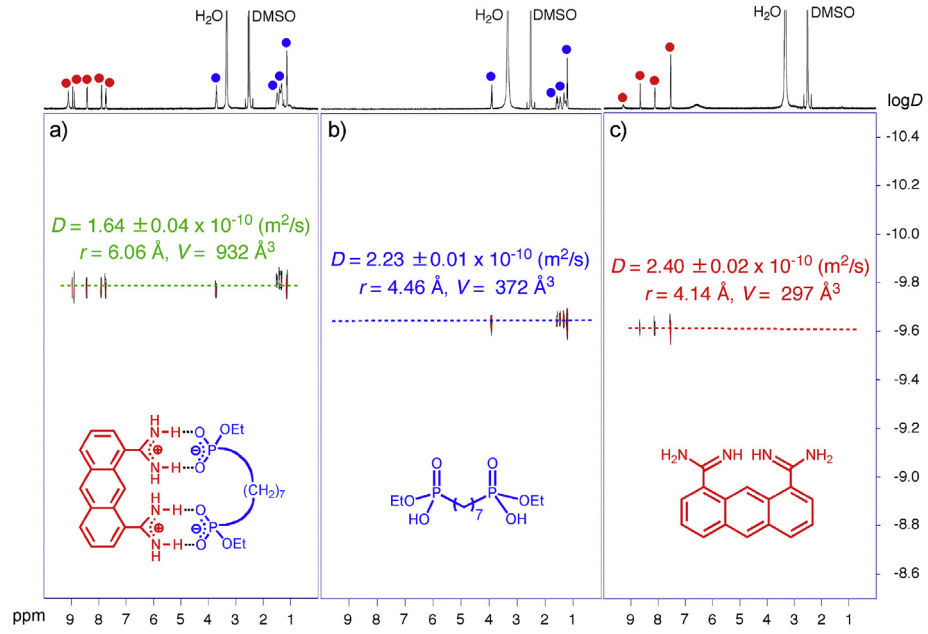

Fig. 4. ^{1}H DOSY spectra (0.95 mM in DMSO-d_6, 298 K, diffusion time Δ = 200 ms) of a) complex **1•2g**, b) diphosphonic acid diethyl ester **2g**, c) diamidine **1**.

Table 2
Comparison of diffusion coefficients, molecular radii and volumes.[a]

Compounds	D (m^2 s^{-1})	r_H (Å)	V (Å^3)
1	2.40 ± 0.02 × 10^{-10}	4.14	297
2c	2.56 ± 0.04 × 10^{-10}	3.88	245
1•2c	1.66 ± 0.01 × 10^{-10}(A)[b]	5.99	900
	1.85 ± 0.01 × 10^{-10}(P)[c]	5.38	652
2d	2.39 ± 0.03 × 10^{-10}	4.16	301
1•2d	1.67 ± 0.05 × 10^{-10}	5.95	882
2f	2.29 ± 0.02 × 10^{-10}	4.34	342
1•2f	1.68 ± 0.05 × 10^{-10}	5.92	869
2g	2.23 ± 0.01 × 10^{-10}	4.46	372
1•2g	1.64 ± 0.04 × 10^{-10}	6.06	932
2h	2.19 ± 0.05 × 10^{-10}	4.54	392
1•2h	1.54 ± 0.02 × 10^{-10}	6.46	1129

[a] Diffusion coefficients were recorded at 298 K in DMSO-d_6 (0.95 mM, diffusion time Δ = 200 ms), and the molecular radii were calculated using the Stokes-Einstein equation.
[b] Derived from diamidine **1**.
[c] Derived from diphosphonic acid diethyl ester **2c**.

diphosphonic acid diethyl esters **2** in a DMSO solution. The diamidine **1** does not show a fluorescence (turn-off state) in the DMSO solution under UV light irradiation due to the PET (photoinduced electron transfer) process[6] from the amidino groups (Scheme 1, Fig. 5). However, after the addition of the diphosphonic acid diethyl esters **2a** (1 equiv.), a blue emission was observed at 440 nm. Similarly, after the addition of the diphosphonic acid diethyl esters **2b**-**2h** (1 equiv.), a blue emission at 432–442 nm was also observed even in the flexible α,ω-diphosphonic acid diethyl esters (Fig. 5). To characterize the origin of these fluorescence spectra, we evaluated the estimated fluorescence wavelengths of **1•2a**, **1•2b** and **1**+2H$^+$ (dissociated amidinium) using the time-dependent density functional theory (TD-DFT, B3LYP/6-31G*//CIS/6-31G*) calculations. The fluorescence wavelengths of the 1:1 complexes **1•2a** (λ_{calc} = 441 nm) and **1•2b** (λ_{calc} = 436 nm) were obtained, and good agreement was observed with the fluorescence wavelengths of **1•2a** (λ_{exp} = 440 nm) and **1•2b** (λ_{exp} = 438 nm) in a DMSO solution (Table 3). The fluorescence wavelength of the dissociate amidinium **1**+2H$^+$ (λ_{calc} = 465 nm, using PCM model in DMSO) was estimated

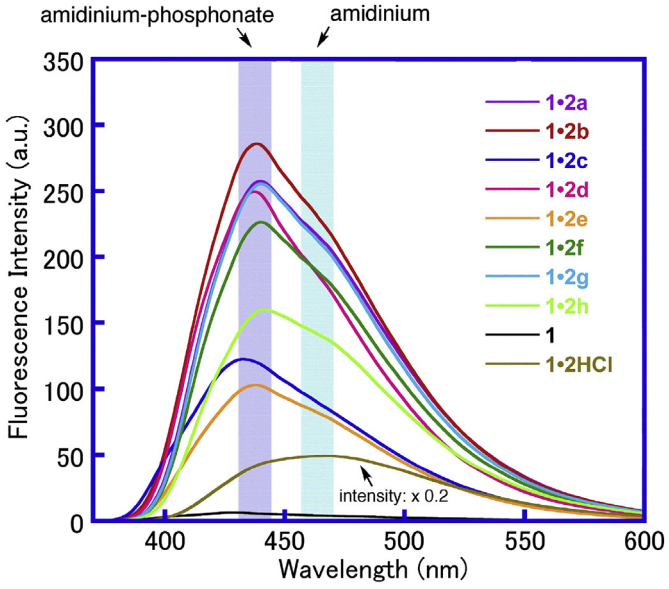

Fig. 5. Fluorescence spectra of diamidine **1** (25 μM in DMSO, λ_{ex} = 348 nm) upon the addition of diphosphonic acid diethyl ester **2a**-**2h** (1 eq.).

from TD-DFT calculation and the fluorescence spectrum of diamidine dihydrochloride **1**•2HCl in DMSO was observed as a broadband around at 460 nm (Fig. 5, Table 3). These observations indicated that complexation of the diamidine **1** with the diphosphonic acid diethyl esters **2** produced stable 1:1 complexes in the DMSO solution even at a low concentration (25 μM) by the formation of two amidinium-phosphonate salt bridges (Scheme 2).

To obtain additional evidence for the formation of the amidinium-phosphonate salt bridge, we measured the fluorescence spectra of **1•2d** (n = 4) after the addition of H_2O (Fig. 6). The fluorescence spectra of **1•2d** was red-shifted (λ_{max} = 460 nm) by the addition of H_2O (0–560 μL), which indicated the formation and dissociation of the amidinium-phosphonate salt bridges in the DMSO solution.

Table 3
Results of TD-DFT calculations and experimental wavelengths for fluorescence spectra.

Compounds	Experimental maximal wavelength (nm)[a]	Calculated maximal wavelength (nm)[b]	Oscillator strength (*f*)[b]
1•2a	440	441	0.08
1•2b	438	436	0.08
1•2H$^+$	—	465[c]	0.12
1•2HCl	460	—	—

[a] Fluorescence spectra were recorded in DMSO (25 μM, λ_{ex} = 348 nm).
[b] TD-PBE0/6-31G*//CIS/6-31G*.
[c] Calculation was performed with PCM model (DMSO).

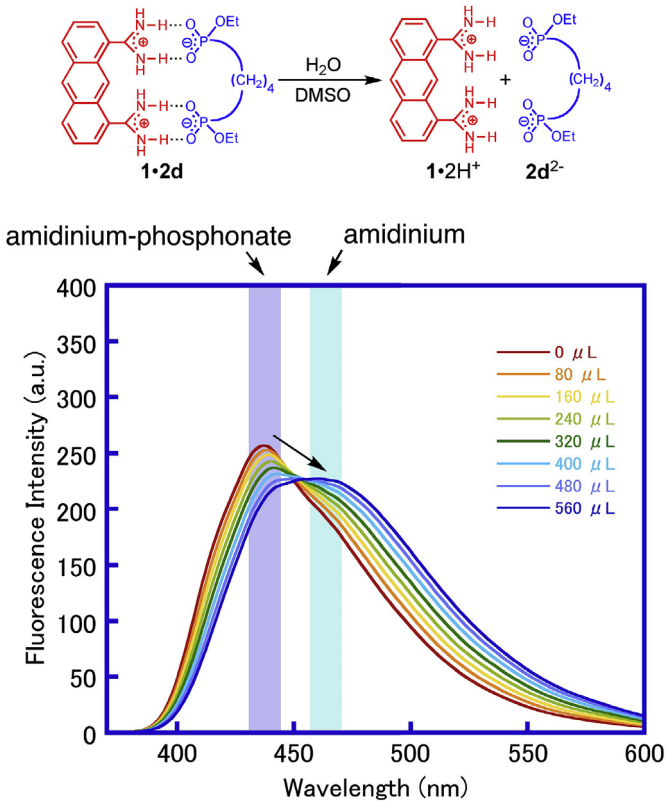

Fig. 6. Fluorescence spectra of **1•2d** (25 μM, DMSO) upon the addition of H_2O (0–560 μL) with excitation at 348 nm.

2.5. Binding experiments of anthracene-based diamidine *1* with monophosphonic acid derivatives

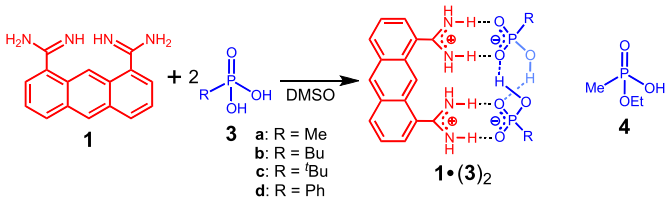

Next, we examined the recognition of the monophosphonic acids with diamidine **1** using fluorescence spectroscopy. According to our previous results about the recognition of the monocarboxylic acids,[5] the formation of the dissociated amidinium **1**•2H$^+$ was observed due to the instability of the formed 1:2 complex. Surprisingly, however, the fluorescence spectra of the diamidine **1** with methylphosphonic acid **3a** (2 equiv.) in DMSO showed a blue

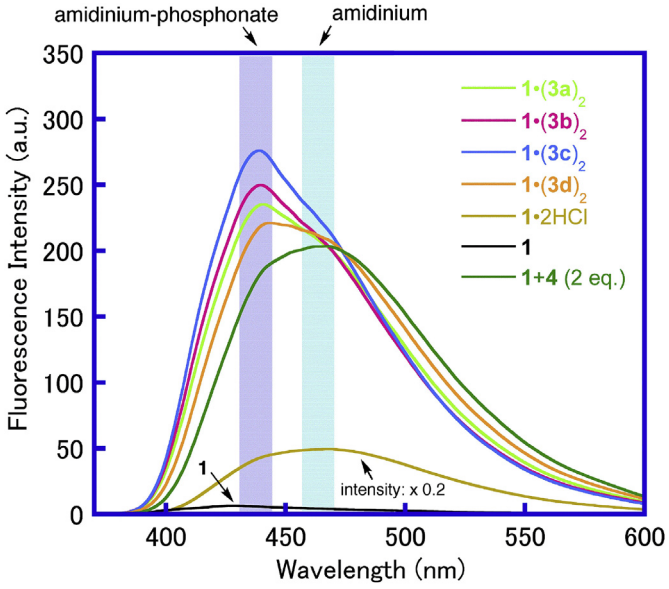

Fig. 7. Fluorescence spectra of diamidine **1** (25 μM in DMSO, λ_{ex} = 348 nm) upon the addition of monophosphonic acids **3a**-**3d** (2 equiv.) and ethyl ester **4** (2 equiv.).

emission band at 441 nm indicating the formation of the stable 1:2 complex (formation of amidinium-phosphonate, Fig. 7). Similar fluorescence spectra were observed for the recognition of the monophosphonic acid **3b** and **3c**, indicating the formation of a stable 1:2 complex. In the recognition of the phenylphosphonic acid **3d**, the fluorescence spectrum showed slightly broad bands and it may have caused the dissociation of the amidinium-phosphonate bonding due to the slightly strong acidity of the phenylphosphonic acid (p$K_{a(calc)}$ = 1.88)[8] compared to the methylphosphonic acid (p$K_{a(calc)}$ = 2.27)[8]. The differences in the recognition ability of the diamidine **1** toward the "monophosphonic acid" and "monocarboxylic acid" may be caused by the presence and absence of an additional hydroxyl group after amidinium-phosphonate and amidinium-carboxylate formation. To clarify this hypothesis, we performed the DFT calculation (B3LYP/6-31G*) of the 1:2 complex of the diamidine **1** and monophosphonic acid **3**. The optimized structure of **1**•(**3a**)$_2$ showed the presence of intermolecular hydrogen bonds of the hydroxyl groups between the two methylphosphonic acids **3a** (Fig. 8). The calculated fluorescence wavelengths of **1**•(**3a**)$_2$ ($\lambda_{obs.}$ = 441 nm, $\lambda_{calc.}$ = 434 nm) and **1**•(**3c**)$_2$ ($\lambda_{obs.}$ = 439 nm, $\lambda_{calc.}$ = 433 nm) using the TD-DFT calculation is very close to the observed fluoresce wavelength, which indicated the formation of the stable complexes **1**•(**3a**)$_2$ and **1**•(**3c**)$_2$ in the DMSO solution (Table S1). To obtain the experimental proof of the formation of the 1:2 complex assisted by the additional intermolecular hydrogen bonding of the phosphonic acids, we examined the recognition of ethyl methylphosphonate **4**, which does not have an additional hydroxyl group on the phosphorous atom after the

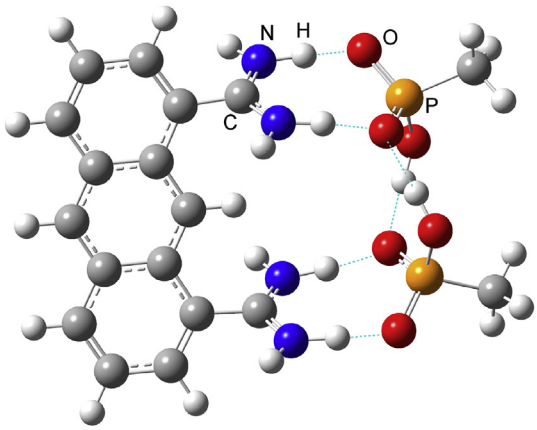

Fig. 8. Optimized structure of **1**•(**3a**)$_2$ at B3LYP/6-31G(d) level.

amidinium-phosphonate formation. After mixing the solution of diamidine **1** and ethyl methylphosphonate **4** (2 equiv.), the broad emission band (λ_{max} = 468 nm) corresponding to the formation of the amidinium **1**•2H$^+$ was observed (Fig. 7). These observations showed that the remaining hydroxyl group of the monophosphonic acid **3** stabilizes the formed 1:2 complex **1**•(**3**)$_2$ (Fig. 8).

To further demonstrate the formation of the 1:2 complex of the diamidine **1** and monophosphonic acid **3**, we measured the ^{1}H NMR and DOSY NMR spectra. The formation of the 1:2 complex **1**•(**3a**)$_2$ (1.89 mM) was achieved by mixing the DMSO-d_6 solution of both components. After the complexation, the ^{1}H NMR spectrum of the obtained solution showed the characteristic upfield and downfield shifts with respect to those of **1** and **3a**, and resonance of the NH protons was also observed at 12.3 and 9.7 ppm which also indicated the formation of the stable complex (Fig. 9 and Fig. S9). However, the two hydrogen atoms for the formation of the intermolecular hydrogen bonding between two phosphonic acids **3** was not observed in the ^{1}H NMR spectrum due to the fast exchanging with a water molecule. Additional proof for the formation of **1**•(**3a**)$_2$ in the solution state was also obtained from the DOSY NMR spectra. The molecular volume of **1**•(**3a**)$_2$ derived from the observed diffusion coefficient (V = 660 Å^3) is slightly greater than the calculated molecular volume of **1**•(**3a**)$_2$ (**1**: V = 280 Å^3, **3a**: V = 99 Å^3, **1**•(**3a**)$_2$: $V_{calc.}$ = 478 Å^3), which indicated the formation of the stable 1:2 complex (Fig. 10, Table 4). The formation of **1**•(**3b**)$_2$ and **1**•(**3c**)$_2$ was also evidenced by the ^{1}H NMR and DOSY NMR spectroscopy (Figs. S10, S11, S31, S32, Table 4). A small difference in the diffusion coefficients derived from **1** and **3d** was observed for the complexation of **1**•(**3d**)$_2$, which indicated that the slightly weak stability of **1**•(**3d**)$_2$, and a similar phenomenon was observed in the fluorescence spectra (Fig. 7). To clarify the effect of the intermolecular hydrogen bonding of the hydroxyl groups on the formation of the stable 1:2 complex **1**•(**3**)$_2$, we measured the DOSY spectrum of the 1:2 mixture of diamidine **1** and ethyl methylphosphonate **4** in the DMSO-d_6 solution. The DOSY spectrum of the desired solution showed two different diffusion signals derived from **1** and **4** (Fig. S34, Table 4). The separately observed DOSY signal for **1**•(**4**)$_2$ showed that the complex exists in equilibrium with the dissociated amidinium and phosphonate fragment. These observations agreed with the difference in the fluorescence spectra of **1**•(**3**)$_2$ and **1**•(**4**)$_2$ (Fig. 7).

The single crystal of the complex **1**•(**3a**)$_2$ was obtained from a CH_3OH solution of the diamidine **1** and methylphosphonic acid **3a** (2 equiv.). The crystal structure of **1**•(**3a**)$_2$ showed the presence of amidinium-phosphonate salt bridges (Fig. S51). The hydrogen atoms in the amidinium-phosphonate bonds were found in the structure (see experimental part), and both are bonded to the nitrogen atoms similar to the amidinium-carboxylate salt bridges. Unfortunately, intermolecular additional hydrogen bonding between two hydroxyl groups of methylphosphonic acid **3a** in the crystal structure of **1**•(**3a**)$_2$ could not be observed. Instead, the intermolecular hydrogen bonding of methylphosphonic acid **3a** and the formation of the one-dimensional network structure of **1**•(**3a**)$_2$

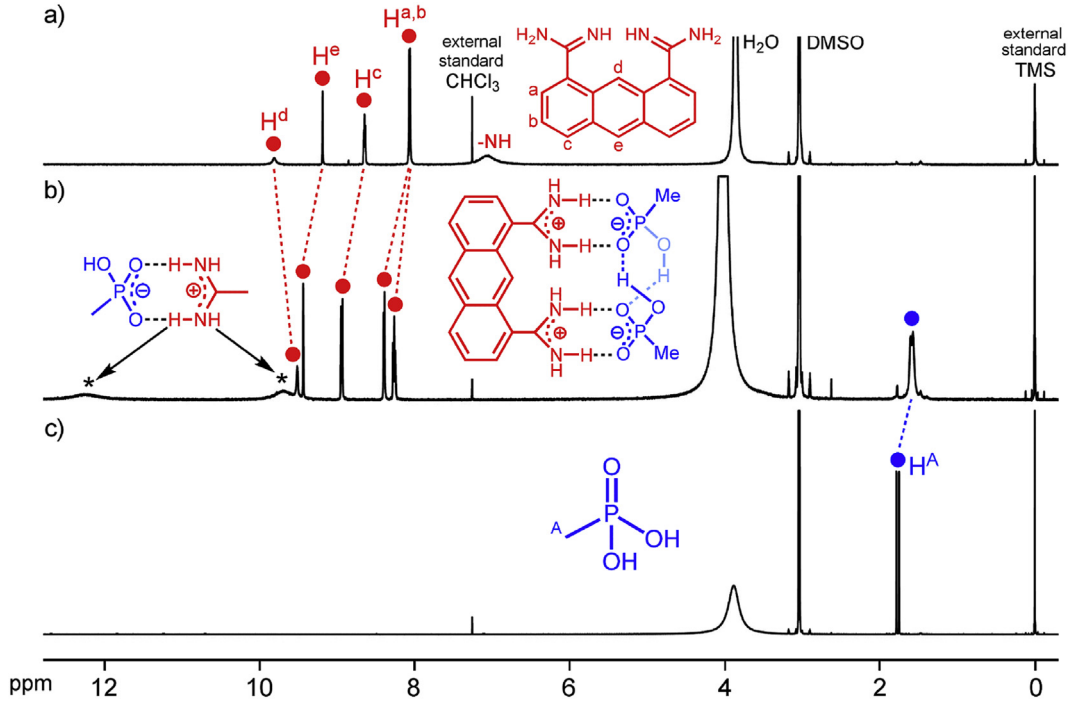

Fig. 9. ^{1}H NMR spectra (1.89 mM in DMSO-d_6, 298 K) of a) diamidine **1**, b) **1**•(**3a**)$_2$ obtained by mixing equimolar solutions of **1** and **3a**, and c) methylphosphonic acid **3a**.

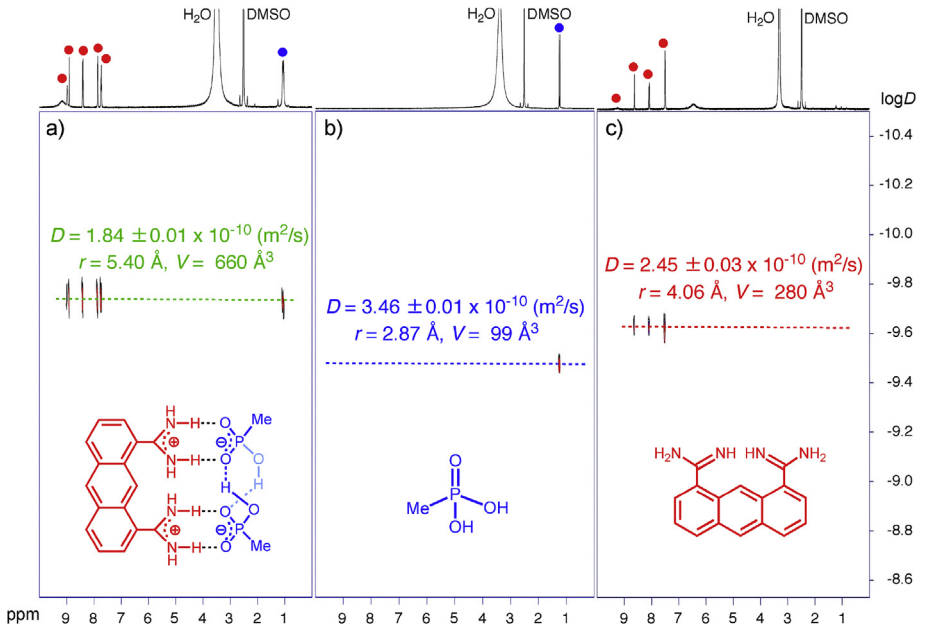

Fig. 10. ^{1}H DOSY spectra (1.89 mM in DMSO-d_6, 298 K, diffusion time Δ = 200 ms) of a) complex **1**•(**3a**)$_2$, b) methylphosphonic acid **3a**, c) diamidine **1**.

Table 4
Comparison of diffusion coefficients, molecular radii and volumes.[a]

Compounds	D (m^2 s^{-1})	r_H (Å)	V (Å^3)
1	2.45 ± 0.03 × 10^{-10}	4.06	280
3a	3.46 ± 0.01 × 10^{-10}	2.87	99
1•(**3a**)$_2$	1.84 ± 0.01 × 10^{-10}	5.40	660
3b	3.08 ± 0.02 × 10^{-10}	3.23	141
1•(**3b**)$_2$	1.71 ± 0.05 × 10^{-10}	5.82	826
3c	3.10 ± 0.01 × 10^{-10}	3.21	139
1•(**3c**)$_2$	1.75 ± 0.03 × 10^{-10}	5.68	768
3d	3.04 ± 0.06 × 10^{-10}	3.27	146
1•(**3d**)$_2$	1.65 ± 0.02 × 10^{-10}(A)[b]	6.03	918
	1.78 ± 0.01 × 10^{-10}(P)[c]	5.59	732
4	4.62 ± 0.05 × 10^{-10}	2.15	42
1•(**4**)$_2$	2.34 ± 0.03 × 10^{-10}(A)[b]	4.25	322
	2.94 ± 0.03 × 10^{-10}(P)[d]	3.38	162

[a] Diffusion coefficients were recorded at 298 K in DMSO-d_6 (1.89 mM, diffusion time Δ = 200 ms), and the molecular radii were calculated using the Stokes-Einstein equation.
[b] Derived from diamidine **1**.
[c] Derived from phosphonic acid **3d**.
[d] Derived from ethyl methylphosphonate **4**.

was observed (Fig. S53). These results support that the formation of the **1**•(**3a**)$_2$ complex having additional intermolecular hydrogen bonding between the two phosphonic acids in the solution state. The single crystal of **1**•(**3c**)$_2$ was also obtained from a CH_3OH solution. The crystal structure of **1**•(**3c**)$_2$ showed a similar one-dimensional network structure, and the pseudo−six-membered ring of the formation of hydrogen bonding between two phosphonic acid **3c** was observed (Figs. S52 and S54). These results support the formation of the **1**•(**3**)$_2$ complex having intermolecular additional hydrogen bonding between the two phosphonic acids **3** in the solution state.

*2.6. Fluorescence titration experiments of diamidine **1** with phosphonic acid derivatives*

The binding constants of the diamidine **1** with diphosphonic acid diethyl esters **2** and monophosphonic acids **3** by fluorescence titrations, and the pK_a values of the monophosphonic acid **3** are summarized in Table 5. The binding constants of the diamidine **1** and diphosphonic acid diethyl esters **2** with a 1:1 stoichiometry are on the order of 10^6 (M^{-1}) in the DMSO solution and slightly higher binding constants were observed compared to the dicarboxylic acid bindings (see ref.[5]). Almost no influence of the chain lengths of the α,β-diphosphonic acid diethyl esters (**2c**-**2h**) on the formation of 1:1 complexes was observed. For the binding of the monophosphonic acids **3**, the binding constants were determined by 1:2 (**1**:**3**) stoichiometry (K_1•K_2/M^{-2}) and almost no influence of the pK_a values of the monophosphonic acid **3** was observed.

To demonstrate the selectivity of the diamidine **1** for the diphosphonic acid **2**, we observed the fluorescence spectra of **1**•**2d** after the addition of acetic acid. The fluorescence spectra of **1**•**2d** were slightly changed by the addition of acetic acid (0−10 equiv.). However, the fluorescence spectra of **1**•**2d** showed a profile sufficient for recognizing the presence of the diphosphonic acid (Fig. S49). These results show that the 1:1 complex of the diamidine **1** and diphosphonic acid **2d** is stabler than the 1:2 complex with acetic acid even in the presence of excess acetic acid. A similar observation was observed for the 1:2 complex **1**•(**3a**)$_2$ (monophosphonic acid) after the addition of acetic acid (Fig. S50).

3. Conclusions

We have investigated the fluorescence detection of the diphosphonic acid and mono-phosphonic acid derivatives using the anthracene-based diamidine **1**. The diamidine **1** forms 1:1 and 1:2 complexes with the di-phosphonic acid and mono-phosphonic acid derivatives, respectively, and showed a blue fluorescence (λ_{em} = 432−442 nm) in the DMSO solution. The formation of amidinium-phosphonate (complex formation) and dissociated amidinum (λ_{em} = 468 nm as a broad band) were distinguished by the difference in the fluorescence wavelength, and confirmed by DOSY NMR spectroscopy and TD-DFT calculations.

Table 5
Binding constants[a] of diamidine **1** with phosphonic acid derivatives and pK_a values of phosphonic acids.

Phosphonic acid derivatives	λ_{em}/nm[b]	K_1/M^{-1}	$K_1 \bullet K_2$[c]/M^{-2}	p*K*a (obs)		p$K_{a\ (calc)}$[f]
2a	441	8.4×10^5				
2b	439	1.6×10^6				
2c (n = 3)	432	1.4×10^6				
2d (n = 4)	438	9.6×10^5				
2e (n = 5)	438	1.0×10^6				
2f (n = 6)	441	1.0×10^6				
2g (n = 7)	440	2.0×10^6				
2h (n = 8)	442	1.6×10^6				
3a (R = Me)	443		1.0×10^{10}	2.41,	7.54[d]	2.27
3b (R = Bu)	442		1.8×10^9			2.66
3c (R = ^{t}Bu)	441		2.7×10^9			3.50
3d (R = Ph)	451		3.5×10^9	1.83,	7.07[e]	1.88

[a] Binding constants were determined by fluorescence titration in DMSO (**1**: 3–25 μM) using the 1:1 and 1:2 models.
[b] Maximum fluorescence wavelength of titration spectra.
[c] The binding constants of the K_1 and K_2 values could not be individually determined.
[d] pK_a values of phosphonic acid in H_2O, taken from ref.[9]
[e] pK_a values of phosphonic acid in H_2O, taken from ref.[10]
[f] Calculated pK_a values of phosphonic acids using Advanced Chemistry Development (ACD/Laboratories) Software V11.02 (1994–2017 ACD/Labs) taken from SciFinder Scholar.

4. Experimental section

4.1. General methods

^{1}H NMR, ^{13}C NMR and ^{31}P NMR spectra were recorded using Avance III 500 (500, 125 and 202 MHz) spectrometers. The FAB-mass spectra were recorded by a JEOL JMS-700 mass spectrometer. The absorption spectra were recorded by a SHIMADZU UV-2550 UV–Visible spectrometer. The fluorescence spectra were recorded by a JASCO FP-6200 spectrometer, and the fluorescence spectra were corrected using rhodamine B as the reference. Infrared spectra were recorded using a Jasco FTIR 4100 spectrometer. All solvents and reagents were purified according to standard procedures. For the NMR measurement using $CDCl_3$, the acidic impurity in the $CDCl_3$ solvent was removed by passage through basic Al_2O_3 (Merck, 101076). Anthracene-based diamidine **1** was prepared by the published procedure.[5]

4.1.1. Synthesis of diphosphonic acid tetraethyl esters (**5**)

General Procedure: The dibromides (6–7 mmol) and triethyl phosphite (10 mL) were stirred and heated to 120 °C for 24 h, then additionally heated to 156 °C (reflux) for 3 h under an argon atmosphere. The consumption of the dibromides was monitored by gas chromatography, and excess triethyl phosphite was removed by short pass vacuum distillation. The residue was purified by column chromatography (AcOEt to AcOEt/MeOH = 10/1) and the corresponding diphosphonic acid tetraethyl esters **5** were obtained.

*4.1.1.1. 1,3-Bis(diethoxyphosphonomethyl)benzene (**5a**).* 92% yield; ^{1}H NMR (500 MHz, $CDCl_3$) δ (ppm) = 7.3–7.2 (m, 4H), 4.1–4.0 (m, 8H), 3.13 (d, $^2J_{P\text{-}H}$ = 21.9 Hz, 4H), 1.25 (t, J = 7.1 Hz, 12H). ^{31}P NMR (202 MHz, $CDCl_3$); δ (ppm) = 26.2.

*4.1.1.2. 1,3-Bis(diethoxyphosphoryl)propane (**5c**).* 93% yield; ^{1}H NMR (500 MHz, $CDCl_3$) δ (ppm) = 4.1–4.0 (m, 8H), 2.0–1.8 (m, 6H), 1.31 (t, J = 7.1 Hz, 12H). ^{31}P NMR (202 MHz, $CDCl_3$); δ (ppm) = 30.5.

*4.1.1.3. 1,4-Bis(diethoxyphosphoryl)butane (**5d**).* 83% yield; ^{1}H NMR (500 MHz, $CDCl_3$) δ (ppm) = 4.1–4.0 (m, 8H), 1.8–1.6 (m, 8H), 1.32 (t, J = 7.1 Hz, 12H). ^{31}P NMR (202 MHz, $CDCl_3$); δ (ppm) = 31.5.

*4.1.1.4. 1,5-Bis(diethoxyphosphoryl)pentane (**5e**).* 87% yield; ^{1}H NMR (500 MHz, $CDCl_3$) δ (ppm) = 4.1–4.0 (m, 8H), 1.76–1.69 (m, 4H), 1.67–1.58 (m, 4H), 1.52–1.47 (m, 2H), 1.32 (t, J = 7.1 Hz, 12H). ^{31}P NMR (202 MHz, $CDCl_3$); δ (ppm) = 32.0.

*4.1.1.5. 1,6-Bis(diethoxyphosphoryl)hexane (**5f**).* 91% yield; ^{1}H NMR (500 MHz, $CDCl_3$) δ (ppm) = 4.09 (m, 8H), 1.76–1.67 (m, 4H), 1.65–1.55 (m, 4H), 1.42–1.38 (m, 4H), 1.32 (t, J = 7.1 Hz, 12H). ^{31}P NMR (202 MHz, $CDCl_3$); δ (ppm) = 32.2.

*4.1.1.6. 1,7-Bis(diethoxyphosphoryl)heptane (**5g**).* 45% yield; ^{1}H NMR (500 MHz, $CDCl_3$) δ (ppm) = 4.1–4.0 (m, 8H), 1.75–1.68 (m, 4H), 1.62–1.57 (m, 4H), 1.40–1.36 (m, 6H), 1.32 (t, J = 7.1 Hz, 12H). ^{31}P NMR (202 MHz, $CDCl_3$); δ (ppm) = 32.2.

*4.1.1.7. 1,8-Bis(diethoxyphosphoryl)octane (**5h**).* 71% yield; ^{1}H NMR (500 MHz, $CDCl_3$) δ (ppm) = 4.1–4.0 (m, 8H), 1.75–1.68 (m, 4H), 1.62–1.55 (m, 4H), 1.4–1.2 (m, 8H), 1.32 (t, J = 7.1 Hz, 12H). ^{31}P NMR (202 MHz, $CDCl_3$); δ (ppm) = 32.5.

*4.1.1.8. 1,3-Bis(diethoxyphosphoryl)benzene (**5b**).* To a solution of 1,3-dibromobenzene (784 mg, 3.32 mmol) and $NiCl_2$ (864 mg, 6.67 mmol) in benzonitrile (30 mL), $P(OEt)_3$ (2.0 mL, 11.5 mmol) was added dropwise over 5 min under argon at 160 °C and stirring was continued for 2 h. The reaction mixture was poured into toluene (50 mL), the organic layer was washed four times with 10% aqueous NH_3, dried over Na_2SO_4 and the solvent evaporated. The remaining benzonitrile was removed under reduced pressure at 60–80 °C. The product **5b** (446 mg, 38%) was isolated after column chromatography (SiO_2, AcOEt to AcOEt/MeOH = 10:1) as a colorless oil. ^{1}H NMR (500 MHz, $CDCl_3$) δ = 8.26–8.20 (m, 1H), 8.02–7.97 (m, 2H), 7.61–7.55 (m, 1H), 4.18–4.07 (m, 8H), 1.34 (t, J = 7.1 Hz, 12H). ^{31}P NMR (202 MHz, $CDCl_3$); δ = 16.8.

4.1.2. Synthesis of bis(hydroxyethoxyphosphoryl) dilithium salts (**6**)

General Procedure: The tetraethyl diphosphonates **5** (1–8 mmol) and LiBr (2.6 eq.) were refluxed in 2-hexanone (10 mL, distilled from K_2CO_3) under an argon atmosphere. After 3 h, the white precipitate was collected by centrifugation and washed five times with Et_2O. The collected precipitate was dried under vacuum to give the dilithium salt **6** as a white powder. Inclusion of excess LiBr in the obtained products was observed by elemental analysis and the products were only characterized by NMR spectroscopy.

*4.1.2.1. 1,3-Bis(hydroxyethoxyphosphorylmethyl)benzene dilithium salt (**6a**).* 82% yield (including LiBr); colorless solid; ^{1}H NMR (500 MHz, D_2O, TMS in $CDCl_3$ as external standard) δ (ppm) = 7.28 (t, J = 7.9 Hz, 1H), 7.18 (brs, 3H), 3.85 (m, 4H), 3.02 (d, $^{2}J_{P\text{-}H}$ = 20.5 Hz, 4H), 1.20 (t, J = 7.1 Hz, 6H). ^{13}C NMR (125 MHz, D_2O, TMS in $CDCl_3$ as external standard) δ (ppm) = 134.9 (m, C_q), 130.8 (t, $^{3}J_{C\text{-}P}$ = 6.3 Hz, CH), 128.5 (CH), 127.3 (t, $^{3}J_{C\text{-}P}$ = 4.4 Hz, CH), 61.3 (d, $^{2}J_{C\text{-}O\text{-}P}$ = 5.0 Hz, OCH_2), 34.2 (d, $^{1}J_{C\text{-}P}$ = 130.0 Hz, CH_2), 16.0 (t, $^{3}J_{C\text{-}O\text{-}P}$ = 3.1 Hz, CH_3). ^{31}P NMR (202 MHz, D_2O, H_3PO_4 in D_2O as external standard); δ (ppm) = 22.9.

*4.1.2.2. 1,3-Bis(hydroxyethoxyphosphoryl)benzene dilithium salt (**6b**).* 95% yield (including LiBr); colorless solid; ^{1}H NMR (500 MHz, D_2O, TMS in $CDCl_3$ as external standard) δ (ppm) = 8.00 (t, J = 12.5 Hz, 1H), 7.87–7.82 (m, 2H), 7.59 (m, 1H), 3.84 (m, 4H), 1.19 (t, J = 7.1 Hz, 6H). ^{13}C NMR (125 MHz, D_2O, TMS in $CDCl_3$ as external standard) δ (ppm) = 133.5 (m, CH),133.4 (dd, $^{1}J_{C\text{-}P}$ = 176.3, $^{3}J_{C\text{-}P}$ = 12.5 Hz, C_q), 133.0 (t, $^{2}J_{C\text{-}P}$ = 10.0 Hz, CH), 128.5 (t, $^{3}J_{C\text{-}P}$ = 13.2 Hz, CH), 61.4 (s, OCH_2), 15.8 (t, $^{3}J_{C\text{-}O\text{-}P}$ = 3.1 Hz, CH_3). ^{31}P NMR (202 MHz, D_2O, H_3PO_4 in D_2O as external standard); δ (ppm) = 14.8.

*4.1.2.3. 1,3-Bis(hydroxyethoxyphosphoryl)propane dilithium salt (**6c**).* 102% yield (including LiBr); colorless solid; ^{1}H NMR (500 MHz, D_2O, TMS in $CDCl_3$ as external standard) δ (ppm) = 3.91 (m, 4H), 1.8–1.6 (m, 6H), 1.25 (t, J = 7.1 Hz, 6H). ^{13}C NMR (125 MHz, D_2O, TMS in $CDCl_3$ as external standard) δ (ppm) = 60.6 (t, $^{2}J_{C\text{-}O\text{-}P}$ = 3.1 Hz, OCH_2), 27.5 (dd, $^{1}J_{C\text{-}P}$ = 133.8, $^{3}J_{C\text{-}P}$ = 15.0 Hz, CH_2), 17.6 (t, $^{2}J_{C\text{-}P}$ = 3.8 Hz, CH_2), 16.0 (t, $^{3}J_{C\text{-}O\text{-}P}$ = 2.5 Hz, CH_3). ^{31}P NMR (202 MHz, D_2O, H_3PO_4 in D_2O as external standard); δ (ppm) = 27.6.

*4.1.2.4. 1,4-Bis(hydroxyethoxyphosphoryl)butane dilithium salt (**6d**).* 102% yield (including LiBr); colorless solid; ^{1}H NMR (500 MHz, D_2O, TMS in $CDCl_3$ as external standard) δ (ppm) = 3.90 (m, 4H), 1.7–1.5 (m, 8H), 1.25 (t, J = 7.1 Hz, 6H). ^{13}C NMR (125 MHz, D_2O, TMS in $CDCl_3$ as external standard) δ (ppm) = 60.5 (d, $^{2}J_{C\text{-}O\text{-}P}$ = 6.3 Hz, OCH_2), 25.9 (d, $^{1}J_{C\text{-}P}$ = 133.8, CH_2), 24.4 (dd, $^{2}J_{C\text{-}P}$ = 18.8, $^{3}J_{C\text{-}P}$ = 4.4 Hz, CH_2), 16.0 (d, $^{3}J_{C\text{-}O\text{-}P}$ = 5.0 Hz, CH_3). ^{31}P NMR (202 MHz, D_2O, H_3PO_4 in D_2O as external standard); δ (ppm) = 28.8.

*4.1.2.5. 1,5-Bis(hydroxyethoxyphosphoryl)pentane dilithium salt (**6e**).* 109% yield (including LiBr); colorless solid; ^{1}H NMR (500 MHz, D_2O, TMS in $CDCl_3$ as external standard) δ (ppm) = 3.90 (m, 4H), 1.7–1.4 (m, 10H), 1.25 (t, J = 7.1 Hz, 6H). ^{13}C NMR (125 MHz, D_2O, TMS in $CDCl_3$ as external standard) δ (ppm) = 60.4 (d, $^{2}J_{C\text{-}O\text{-}P}$ = 6.3 Hz, OCH_2), 31.7 (t, $^{3}J_{C\text{-}P}$ = 16.3 Hz, CH_2), 26.1 (d, $^{1}J_{C\text{-}P}$ = 133.8, CH_2), 22.5 (d, $^{2}J_{C\text{-}P}$ = 5.0 Hz, CH_2), 16.0 (d, $^{3}J_{C\text{-}O\text{-}P}$ = 6.3 Hz, CH_3). ^{31}P NMR (202 MHz, D_2O, H_3PO_4 in D_2O as external standard); δ (ppm) = 29.2.

*4.1.2.6. 1,6-Bis(hydroxyethoxyphosphoryl)hexane dilithium salt (**6f**).* 109% yield (including LiBr); colorless solid; ^{1}H NMR (500 MHz, D_2O, TMS in $CDCl_3$ as external standard) δ (ppm) = 3.89 (m, 4H), 1.62–1.55 (m, 4H), 1.55–1.49 (m, 4H), 1.38 (m, 4H), 1.26 (t, J = 7.1 Hz, 6H). ^{13}C NMR (125 MHz, D_2O, TMS in $CDCl_3$ as external standard) δ (ppm) = 60.4 (d, $^{2}J_{C\text{-}O\text{-}P}$ = 5.0 Hz, OCH_2), 29.9 (d, $^{3}J_{C\text{-}P}$ = 17.5 Hz, CH_2), 26.1 (d, $^{1}J_{C\text{-}P}$ = 133.8, CH_2), 22.8 (d, $^{2}J_{C\text{-}P}$ = 5.0 Hz, CH_2), 16.0 (d, $^{3}J_{C\text{-}O\text{-}P}$ = 5.0 Hz, CH_3). ^{31}P NMR (202 MHz, D_2O, H_3PO_4 in D_2O as external standard); δ (ppm) = 29.4.

*4.1.2.7. 1,7-Bis(hydroxyethoxyphosphoryl)heptane dilithium salt (**6g**).* 99% yield (including LiBr); colorless solid; ^{1}H NMR (500 MHz, D_2O, TMS in $CDCl_3$ as external standard) δ (ppm) = 3.89 (m, 4H), 1.62–1.55 (m, 4H), 1.55–1.46 (m, 4H), 1.40–1.32 (m, 6H), 1.25 (t, J = 7.1 Hz, 6H). ^{13}C NMR (125 MHz, D_2O, TMS in $CDCl_3$ as external standard) δ (ppm) = 60.4 (d, $^{2}J_{C\text{-}O\text{-}P}$ = 5.0 Hz, OCH_2), 30.1 (d, $^{3}J_{C\text{-}P}$ = 16.3 Hz, CH_2), 28.0 (s, CH_2), 26.2 (d, $^{1}J_{C\text{-}P}$ = 132.5, CH_2), 22.8 (d, $^{2}J_{C\text{-}P}$ = 3.8 Hz, CH_2), 16.0 (d, $^{3}J_{C\text{-}O\text{-}P}$ = 5.0 Hz, CH_3). ^{31}P NMR (202 MHz, D_2O, H_3PO_4 in D_2O as external standard); δ (ppm) = 29.5.

*4.1.2.8. 1,8-Bis(hydroxyethoxyphosphoryl)octane dilithium salt (**6h**).* 104% yield (including LiBr); colorless solid; ^{1}H NMR (500 MHz, D_2O, TMS in $CDCl_3$ as external standard) δ (ppm) = 3.89 (m, 4H), 1.61–1.53 (m, 4H), 1.53–1.46 (m, 4H), 1.37–1.29 (m, 8H), 1.25 (t, J = 7.1 Hz, 6H). ^{13}C NMR (125 MHz, D_2O, TMS in $CDCl_3$ as external standard) δ (ppm) = 60.4 (d, $^{2}J_{C\text{-}O\text{-}P}$ = 5.0 Hz, OCH_2), 30.3 (d, $^{3}J_{C\text{-}P}$ = 17.5 Hz, CH_2), 28.3 (s, CH_2), 26.2 (d, $^{1}J_{C\text{-}P}$ = 132.5, CH_2), 22.86 (d, $^{2}J_{C\text{-}P}$ = 5.0 Hz, CH_2), 16.0 (d, $^{3}J_{C\text{-}O\text{-}P}$ = 6.3 Hz, CH_3). ^{31}P NMR (202 MHz, D_2O, H_3PO_4 in D_2O as external standard); δ (ppm) = 29.6.

*4.1.3. Synthesis of diphosphonic acid P,P′-diethyl esters (**2**)*

General Procedure: An ion exchange resin of sulfonic acid (6 g, Dowex 50Wx8 200–400 mesh) was activated with 6 M HCl (25 mL), then washed with distilled water (30 mL) in a disposable column (16 × 80 mm). An aqueous solution (5 mL) of the bis(hydroxyethoxyphosphoryl) dilithium salts **6** (ca 50 mg, 0.15–0.19 mmol) was deposited on the resin and eluted with distilled water (ca 50 mL) until the eluent become neutral (pH = 7). The eluent was concentrated in vacuo and the residue was continuously evacuated under vacuum for one week. The purity of the obtained diphosphonic acid diethyl esters **2** was analyzed by the ^{1}H NMR integral ratio in comparison with the internal standards.

*4.1.3.1. 1,3-Bis(hydroxyethoxyphosphorylmethyl)benzene (**2a**).* Colorless oil; 94% yield; ^{1}H NMR (500 MHz, DMSO-d_6) δ (ppm) = 7.21 (t, J = 7.5 Hz, 1H), 7.13–7.11 (m, 3H), 3.88 (m, 4H), 3.02 (d, $^{1}J_{P\text{-}H}$ = 21.6 Hz, 4H), 1.16 (t, J = 7.0 Hz, 6H). ^{13}C NMR (125 MHz, DMSO-d_6) δ (ppm) = 133.1 (m, C_q), 131.1 (t, $^{3}J_{C\text{-}P}$ = 6.3 Hz, CH), 127.8 (CH), 127.3 (m, CH), 60.5 (d, $^{2}J_{C\text{-}O\text{-}P}$ = 5.0 Hz, OCH_2), 33.6 (d, $^{1}J_{C\text{-}P}$ = 132.5 Hz, CH_2), 16.3 (t, $^{3}J_{C\text{-}O\text{-}P}$ = 6.3 Hz, CH_3). ^{31}P NMR (202 MHz, DMSO-d_6); δ (ppm) = 23.7; HRMS (FAB, NBA) m/z = 345.0631 (calculated for $[M+Na]^+$: 345.0633); IR (KBr, cm^{-1}): ν 3389, 2985, 2911, 2360, 2336, 1700, 1167, 1038.

*4.1.3.2. 1,3-Bis(hydroxyethoxyphosphoryl)benzene (**2b**).* Colorless oil; 69% yield; ^{1}H NMR (500 MHz, DMSO-d_6) δ (ppm) = 8.01 (t, $^{3}J_{P\text{-}H}$ = 12.9 Hz, 1H), 7.85 (m, 2H), 7.63 (m, 1H), 3.91 (m, 4H), 1.18 (t, J = 7.1 Hz, 6H). ^{13}C NMR (125 MHz, DMSO-d_6) δ (ppm) = 133.9 (m, CH), 133.4 (t, $^{2}J_{C\text{-}P}$ = 10.0 Hz, CH), 131.7 (dd, $^{1}J_{C\text{-}P}$ = 181.3, $^{3}J_{C\text{-}P}$ = 12.5 Hz, C_q), 128.7 (t, $^{3}J_{C\text{-}P}$ = 13.1 Hz, CH), 60.8 (s, OCH_2), 16.2 (s, CH_3). ^{31}P NMR (202 MHz, DMSO-d_6); δ (ppm) = 14.1; HRMS (FAB, NBA) m/z = 238.9866 (calculated for $[M+H]^+$: 238.9874); IR (KBr, cm^{-1}): ν 3463, 2987, 2908, 2360, 2335, 1699, 1166, 1112, 1032.

*4.1.3.3. 1,3-Bis(hydroxyethoxyphosphoryl)propane (**2c**).* 91% yield; colorless oil; ^{1}H NMR (500 MHz, DMSO-d_6) δ (ppm) = 3.90 (m, 4H), 1.8–1.6 (m, 6H), 1.20 (t, J = 7.1 Hz, 6H). ^{13}C NMR (125 MHz, DMSO-d_6) δ (ppm) = 59.8 (t, $^{2}J_{C\text{-}O\text{-}P}$ = 2.5 Hz, CH_2), 26.5 (dd, $^{1}J_{C\text{-}P}$ = 136.3, $^{3}J_{C\text{-}P}$ = 15.0 Hz, CH_2), 16.5 (t, $^{2}J_{C\text{-}P}$ = 4.4 Hz, CH_2), 16.4 (t, $^{3}J_{C\text{-}O\text{-}P}$ = 3.1 Hz, CH_3). ^{31}P NMR (202 MHz, DMSO-d_6); δ (ppm) = 28.5; HRMS (FAB, NBA) m/z = 283.0476 (calculated for $[M+Na]^+$: 283.0476); IR (KBr, cm^{-1}): ν 3464, 2985, 2911, 2360, 2335, 1699, 1204, 1165, 1043, 997.

*4.1.3.4. 1,4-Bis(hydroxyethoxyphosphoryl)butane (**2d**).* 87% yield; colorless waxy solid; ^{1}H NMR (500 MHz, DMSO-d_6) δ = 3.89 (m, 4H), 1.62–1.47 (m, 8H), 1.18 (t, J = 7.1 Hz, 6H). ^{13}C NMR (125 MHz, DMSO-d_6) δ (ppm) = 59.9 (d, $^{2}J_{C\text{-}O\text{-}P}$ = 6.3 Hz, CH_2), 25.5 (d, $^{1}J_{C\text{-}P}$ = 137.5 Hz, CH_2), 23.4 (dd, $^{2}J_{C\text{-}P}$ = 5.0 Hz, $^{3}J_{C\text{-}P}$ = 16.3 Hz, CH_2), 16.4 (d, $^{3}J_{C\text{-}O\text{-}P}$ = 6.3 Hz, CH_3). ^{31}P NMR (202 MHz, DMSO-d_6); δ = 29.2; HRMS (FAB, NBA) m/z = 297.0637 (calculated for $[M+Na]^+$:

297.0633); IR (KBr, cm^{-1}): ν 3427, 2993, 2946, 2910, 2364, 2340, 1682, 1241, 1191, 1165, 1042, 992, 967.

*4.1.3.5. 1,5-Bis(hydroxyethoxyphosphoryl)pentane (**2e**).* 93% yield; colorless waxy solid; ^1H NMR (500 MHz, DMSO-d_6) δ (ppm) = 3.90 (m, 4H), 1.59–1.52 (m, 4H), 1.49–1.39 (m, 6H), 1.20 (t, J = 7.1 Hz, 6H). ^{13}C NMR (125 MHz, DMSO-d_6) δ (ppm) = 59.8 (d, $^2J_{C\text{-}O\text{-}P}$ = 6.3 Hz, CH_2), 30.7 (t, $^3J_{C\text{-}P}$ = 15.6 Hz, CH_2), 25.6 (d, $^1J_{C\text{-}P}$ = 137.5, CH_2), 22.0 (d, $^2J_{C\text{-}P}$ = 5.0 Hz, CH_2), 16.4 (d, $^3J_{C\text{-}O\text{-}P}$ = 6.3 Hz, CH_3). ^{31}P NMR (202 MHz, DMSO-d_6); δ (ppm) = 29.3; HRMS (FAB, NBA) m/z = 311.0792 (calculated for $[M+Na]^+$: 311.0789); IR (KBr, cm^{-1}): ν 3444, 2985, 2944, 2871, 2363, 2340, 1682, 1247, 1188, 1042, 982.

*4.1.3.6. 1,6-Bis(hydroxyethoxyphosphoryl)hexane (**2f**).* 75% yield; colorless waxy solid; ^1H NMR (500 MHz, DMSO-d_6) δ (ppm) = 3.90 (m, 4H), 1.61–1.52 (m, 4H), 1.49–1.39 (m, 4H), 1.36–1.29 (m, 4H), 1.20 (t, J = 7.1 Hz, 6H). ^{13}C NMR (125 MHz, DMSO-d_6) δ (ppm) = 59.8 (d, $^2J_{C\text{-}O\text{-}P}$ = 5.0 Hz, CH_2), 29.4 (d, $^3J_{C\text{-}P}$ = 16.3 Hz, CH_2), 25.7 (d, $^1J_{C\text{-}P}$ = 137.5, CH_2), 22.2 (d, $^2J_{C\text{-}P}$ = 5.0 Hz, CH_2), 16.4 (d, $^3J_{C\text{-}O\text{-}P}$ = 6.3 Hz, CH_3). ^{31}P NMR (202 MHz, DMSO-d_6); δ (ppm) = 29.4; HRMS (FAB, NBA) m/z = 325.0948 (calculated for $[M+Na]^+$: 325.0946); IR (KBr, cm^{-1}): ν 3427, 2991, 2939, 2864, 2362, 2339, 1652, 1234, 1187, 1036, 986, 965.

*4.1.3.7. 1,7-Bis(hydroxyethoxyphosphoryl)heptane (**2g**).* 87% yield; colorless waxy solid; ^1H NMR (500 MHz, DMSO-d_6) δ (ppm) = 3.90 (m, 4H), 1.61–1.52 (m, 4H), 1.50–1.39 (m, 4H), 1.35–1.28 (m, 4H), 1.28–1.22 (m, 2H), 1.20 (t, J = 7.1 Hz, 6H). ^{13}C NMR (125 MHz, DMSO-d_6) δ (ppm) = 59.8 (d, $^2J_{C\text{-}O\text{-}P}$ = 5.0 Hz, CH_2), 29.7 (d, $^3J_{C\text{-}P}$ = 15.0 Hz, CH_2), 28.2 (s, CH_2), 25.8 (d, $^1J_{C\text{-}P}$ = 136.3, CH_2), 22.4 (d, $^2J_{C\text{-}P}$ = 3.8 Hz, CH_2), 16.4 (d, $^3J_{C\text{-}O\text{-}P}$ = 6.3 Hz, CH_3). ^{31}P NMR (202 MHz, DMSO-d_6); δ (ppm) = 29.5; HRMS (FAB, NBA) m/z = 339.1115 (calculated for $[M+Na]^+$: 339.1102); IR (KBr, cm^{-1}): ν 3445, 2984 2932, 2864, 2362, 2339, 1683, 1653, 1245, 1186, 1049, 984.

*4.1.3.8. 1,8-Bis(hydroxyethoxyphosphoryl)octane (**2h**).* 86% yield; colorless waxy solid; ^1H NMR (500 MHz, DMSO-d_6) δ (ppm) = 3.89 (m, 4H), 1.60–1.51 (m, 4H), 1.50–1.39 (m, 4H), 1.35–1.28 (m, 4H), 1.26–1.22 (m, 4H), 1.19 (t, J = 7.1 Hz, 6H). ^{13}C NMR (125 MHz, DMSO-d_6) δ (ppm) = 59.8 (d, $^2J_{C\text{-}O\text{-}P}$ = 5.0 Hz, CH_2), 29.9 (d, $^3J_{C\text{-}P}$ = 16.3 Hz, CH_2), 28.4 (s, CH_2), 25.8 (d, $^1J_{C\text{-}P}$ = 136.3, CH_2), 22.4 (d, $^2J_{C\text{-}P}$ = 5.0 Hz, CH_2), 16.4 (d, $^3J_{C\text{-}O\text{-}P}$ = 5.0 Hz, CH_3). ^{31}P NMR (202 MHz, DMSO-d_6); δ (ppm) = 29.4; HRMS (FAB, NBA) m/z = 353.1269 (calculated for $[M+Na]^+$: 353.1259); IR (KBr, cm^{-1}): ν 3463, 2986, 2926, 2849, 2361, 2338, 1671, 1119, 1048, 998.

4.2. Jobs plot analysis (fluorescence spectroscopy)

The stock solutions of **1** and phosphonic acids (**2**, **3**) in DMSO (1.0–15 mM) were prepared in separate volumetric flasks. Several sample solutions containing both the diamidine **1** and phosphonic acids in different ratios (1/9 to 9/1) were prepared and maintained at 0.2 mM. The fluorescence spectra of the mixtures were recorded, and the intensities were analyzed by Job's method.

4.3. DOSY measurements

The ^1H DOSY experiments were carried out at 298 K using a Bruker Avance III 500 MHz spectrometer equipped with a 5-mm BBFO probe with a z-axis gradient coil. Data were acquired and processed using the Bruker TopSpin 3.0 software. A series of diffusion ordered spectra were collected of the samples using the LEDbp pulse sequence.[11] The pulse-fields were incremented in 50 steps from 2% to 95% of the maximum gradient strength in a linear ramp. The gradient length was selected between 2.0 and 3.0 ms with a diffusion time of 200 ms and an eddy current delay of 5 ms.

4.4. Fluorescence titrations

A solution of the diamidine **1** was prepared (3–25 μM in DMSO), and an aliquot (3 mL) was transferred to a 1-cm fluorescence tube. To this solution was dropwise added a stock solution of the phosphonic acid (0.6–5 mM in DMSO) in small portions. The fluorescence spectra were recorded by excitation at 348 nm. The association constants were calculated using the program HYPSPEC[12] and are summarized in Table 5.

4.5. Computational methods

The ground-state geometries were fully optimized using the density functional theory (DFT) with the B3LYP hybrid functional at the basis set level of 6-31G*. The excited-state geometries were optimized by the ab-initio configuration interaction singles method (CIS/6-31G*); the frequency calculations allowed verification that those structures did not present imaginary frequencies and we had global minima. With this optimized geometry, we calculated the emission spectrum in the time-dependent density functional theory (TD-DFT) with the B3LYP functional at the 6-31G* basis set level.[13,14] All of the calculations were performed with Gaussian 09 W.[15]

4.6. Crystallographic analysis

Crystals suitable for X-ray crystallography were grown from the solutions of **1**•(**3a**)$_2$ and **1**•(**3c**)$_2$ in MeOH that were stored in a small vial and left to stand in the sample bottle in the presence of molecular sieves 4A for several days. For the crystallographic data collection, a Rigaku AFC-7R with graphite-monochromated Cu-Kα radiation was used. Calculations were performed using the Crystal Structure 3.8 crystallographic software package.[16] The crystal structures were solved by a direct method using Shelxs-97[17], and the structure refinements were performed by a full-matrix least squares methods using Shelx-97. Details of the data are summarized in Table S2. All non-hydrogen atoms were anisotropically refined. The hydrogen atoms of the amidino groups were located in a difference Fourier map and were isotropically refined. All the other hydrogen atoms were placed in idealized positions and were included in structure factor calculations, but were not refined. CCDC-1582835 and -1582836 contain the supplementary crystallographic data for this paper. These data can be obtained free of charge from The Cambridge Crystallographic Data Centre via www.ccdc.cam.ac.uk/data request/cif.

Acknowledgments

This study was supported in part by the Kyoto Institute of Technology Research Fund. We thank Prof. T. Harada (Kyoto Institute of Technology) for his helpful discussions.

Appendix A. Supplementary data

Supplementary data related to this article can be found at https://doi.org/10.1016/j.tet.2017.12.011.

References

1. (a) Hargrove AE, Nieto S, Zhang T, Sessler JL, Anslyn EV. *Chem Rev*. 2011;111:6603. and references cited therein;
(b) Lee S, Yuen KKY, Jolliffe KA, Yoon J. *Chem Soc Rev*. 2015;44:1749;

(c) Zhang D, Cochrane JR, Martinez A, Gao G. *RSC. Adv.* 2014;4, 29735.
2. (a) Esipenko NA, Koutnik P, Minami T, et al. *Chem Sci*. 2013;4:3617;
(b) Liu Y, Bonizzoni M. *J Am Chem Soc*. 2014;136, 14223.
3. (a) Horsman GP, Zechel DL. *Chem Rev*. 2017;117:5704;
(b) Nowack B. *Water Res*. 2003;37:2533;
(c) Mukherjee S, Huang C, Guerra F, Wang K, Oldfield E. *J Am Chem Soc*. 2009;131:8374. and references cited therein.
4. (a) Ward MD. *Chem Commun*. 2005:5838;
(b) Lie S, Maris T, Wuest JD. *Cryst Growth Des*. 2014;14:3658.
5. Kusukawa T, Toyama K, Takeshita S, Tanaka S. *Tetrahedron*. 2012;68:9973.
6. Andréasson J, Pischel U. *Chem Soc Rev*. 2010;39:174.
7. The observed molecular volume from the DOSY spectroscopy for the formed comlexes is depending on the structure shape and rigidity of the formed complex. Slightly larger volume of the formed complex **1•2a** was observed compared to the sum of the volumes of the free building blocks **1** and **2a**. It may cause the steric effects of the outward two P-OEt groups and formation of inner void space of **1•2a** (see the structure in Figure 2a).
8. Calculated pK_a values of monophosphonic acids using Advanced Chemistry Development (ACD/Laboratories) Software V11.02 (1994-2017 ACD/Labs) taken from SciFinder Scholar.
9. Abbott A, Sierakowski T, Kiddle JJ, Clark KK, Mezyk SP. *J Phys Chem B*. 2010;114:7681.
10. Jaffe HH, Freedman LD, Doak GO. *J Am Chem Soc*. 1953;75:2209.
11. Wu D, Chen A, Johnson Jr CS. *J Magn Reson A*. 1995;115:260.
12. Gans P, Sabatini A, Vacca A. *Talanta*. 1996;43:1739.
13. Barraza-Jimenez D, Flores-Hidalgo A, Glossman-Mitnik D. *THEOCHEM*. 2009;894:64.
14. Yang B, Kim SK, Xu H, et al. *ChemPhysChem*. 2008;9:2601.
15. Frisch MJ, Trucks GW, Schlegel HB, et al. *Gaussian 09, Revision C.01*. Wallingford CT: Gaussian, Inc.; 2010.
16. CrystalStructure 3.8, Crystal Structure Analysis Package, Rigaku and Rigaku/MSC, 9009 New Trails Dr. The Woodlands TX 77381 USA, 2000-2006.
17. Sheldrick GM. *Acta Crystallogr A*. 2008;64:112.